Plasma Chemistry and Plasma Processing (2020) 40:99–117
https://doi.org/10.1007/s11090-019-10037-2

ORIGINAL PAPER

Miniature Non-thermal Plasma Induced Cell Cycle Arrest and Apoptosis in Lung Carcinoma Cells

Surya B. Karki[1] · Tripti Thapa Gupta[1] · Eda Yildirim-Ayan[1,2] · Kathryn M. Eisenmann[3] · Halim Ayan[1,4]

Received: 24 March 2019 / Accepted: 30 September 2019 / Published online: 14 October 2019

Abstract

Non-thermal plasma has been a promising new cancer treatment modality in plasma oncology field. It generates extracellular and intracellular reactive species which are key factors for the treatment of cancer cells. In this study, we investigated the differential effect of non-thermal plasma on both A549 lung adenocarcinoma and MRC-5 lung fibroblast cells. Extracellular generation of reactive species in both A549 lung cancer and MRC-5 normal lung fibroblast cells were similar, whereas intracellular penetration of reactive species generated by plasma in A549 cancer cells were almost fourfold higher than the normal cells. Interestingly, A549 cancer cells treated for shorter (15 and 30 s) and longer durations (60 and 120 s) get arrested in S-phase (19%) and G2/M phase (28%) respectively. In a healthy MRC-5 cells, few cells arrested in S and G2/M phase in relative to A549 cells for all treatment time. Finally, we evaluated the expression of apoptosis-related genes, H2AX, BAX, P53, Caspase-8, and ATM on normal and cancer cells. There was a higher expression of BAX gene for 120 s plasma treated A549 cell samples at day 1 relative to MRC-5 cells. These findings demonstrate that non-thermal plasma generated reactive species creates intracellular stress, that arrests cell cycle and induces apoptosis in cancer cells. This study suggests that non-thermal plasma could be a potential therapy for lung cancer treatment.

Keywords Non-thermal plasma · Lung cancer · Gene expression · Apoptosis · Cell cycle

✉ Halim Ayan
halim.ayan@utoledo.edu

[1] Department of Bioengineering, College of Engineering, University of Toledo, Toledo, OH 43606, USA

[2] Department of Orthopaedic Surgery, University of Toledo Medical Center, Toledo, OH 43614, USA

[3] Department of Cancer Biology, University of Toledo Health Science Campus, Toledo, OH 43614, USA

[4] Department of Mechanical, Industrial, and Manufacturing Engineering, College of Engineering, University of Toledo, Toledo, OH 43606, USA

Introduction

According to the American Lung Association, lung cancer is one of the major cancer-related deaths worldwide and in the United States [1, 2]. Radiotherapy, chemotherapy, and surgery are commonly used treatment techniques for lung cancer, yet these modalities have pitfalls including radiation, development of chemo resistance and damaging healthy cells. Therefore, there is a great demand to develop innovative therapeutics method that can selectively kill the cancer cells while preserving the healthy cells function [1, 3]. Non-thermal plasma could be an alternative anti-cancer modality alone or together with other chemo-drugs for metastatic lung cancers due to its selective nature of killing cancer cells [4].

Non-thermal plasma generates different reactive oxygen species (ROS) and reactive nitrogen species (RNS) such as nitrate (NO_3), hydrogen peroxide (H_2O_2), singlet oxygen, ozone, and hydroxyl radicals [5–9]. The Non-thermal Plasma generated ROS and RNS have been reported to impair intracellular structures such as DNA and mitochondria, leading to cancer cell apoptosis [10, 11]. The research published by Kalghatgi et al. [12], studied the effect of non-thermal plasma on breast epithelial cells and showed increased double-strand DNA breakage. Similarly, Blackert et al. [13] demonstrated the linear increase of DNA damage in human keratinocytes (HaCaT) cells due to non-thermal plasma. Another research by Hirst et al. [14] demonstrated high levels of DNA damage in prostate epithelial cells in response to non-thermal plasma. Moreover, Kwon et al. [15] studied the cytotoxic effects of non-thermal plasma in cervical cancer cells. They demonstrated the selective inhibition of cancer cell proliferation along with apoptotic death induced by plasma in a dose-dependent manner. Also, Liedtke et al. [16] demonstrated the decreased cell viability and proliferation of pancreatic cancer cells in response to non-thermal plasma, whereas mouse fibroblasts were less affected. And the other research group by Nakamura et al. [17] showed non-thermal plasma activated medium inhibited metastasis of ovarian cancer cells. While many researches have studied the effect of plasma on DNA damage in cancer cells, most studies lack normal cellular control. Also, these studies did not assess normal cell responses along with tumor cell responses.

In our prior studies, we discovered that non-thermal plasma treatment decreased cell viability, and induced apoptosis in A549 lung cancer cells embedded within 3D collagen matrix [3]. Moreover, our plasma system was also able to inhibits the migration of cancer cells [18]. Thus, in this study, unlike other studies, we investigated the viability effects of non-thermal plasma generated by our designed and fabricated miniature dielectric barrier discharge (DBD) plasma system on adenocarcinoma epithelial cells (A549) and normal lung fibroblast cells (MRC-5) embedded within 3D collagen matrix. In addition, we studied the changes in intracellular and extracellular reactive species upon plasma treatment on monolayer cells. Further, we assessed the effect of plasma on the viability of lung cancer and fibroblast cells, cell cycle arrest, and expression of apoptosis-related genes. Similar study was done by Georgescu et al. [19] where they studied the effects of plasma apoptosis between tumoral (colon carcinoma and melanoma cells) and normal cells (macrophages).

Based on our previous findings, we hypothesized that plasma treatment induces apoptosis in cancer cells, and not in normal cells. To test this hypothesis, we cultured A549 lung cancer cells and MRC5 normal healthy lung cells in two different culture media. Although both cells lines are genetically, morphologically and functionally different we wanted to compare the effects of plasma on both healthy and cancerous cell line to observe the differential effects in cell viability cell cycle and cell apoptosis. We analyzed the gene expression

associated with apoptosis such as BAX, p53, Caspase-8, and ATM in both normal and cancer lung cells in response to non-thermal plasma. Our results showed that plasma arrest the cell cycle of A549 cancer cells at G2/M phase at higher treatment time (60 and 120 s). Furthermore, the percentage of cells arrested at G2/M phase for MRC-5, is relatively lower than A549 cells. This suggests that plasma possess detrimental effect to the cancer cells, while supporting the normal cell viability.

Materials and Methods

Miniature Non-thermal Plasma Design

The miniature dielectric barrier discharge (DBD) plasma device was designed, manufactured and characterized in our lab [18]. Briefly, it consists of a copper electrode (1.2 mm diameter) that is inserted at the center of the hollow cylindrical shaped nonconductive insulator of 4 cm in length and 5.5 mm diameter. The insulator along with copper electrode is inserted in the 6 mm diameter test-tube. The lower end of the test-tube with thickness of 0.5 mm act as the dielectric barrier (Fig. 1). In this study, in order to generate the non-thermal plasma, high voltage of 12 kV is applied at 1000 Hz with 10 µs pulse width and 1 µs rise and fall time. On applying high voltage, a visible plasma discharge is produced in ambient air.

Cell Culture and Fabrication of Cell Encapsulated 3D Collagen Matrix

Human lung adenocarcinoma epithelial cells (A549; ATCC) and human fetal lung fibroblasts cells (MRC-5; ATCC) were used for this research and both cells lines were grown

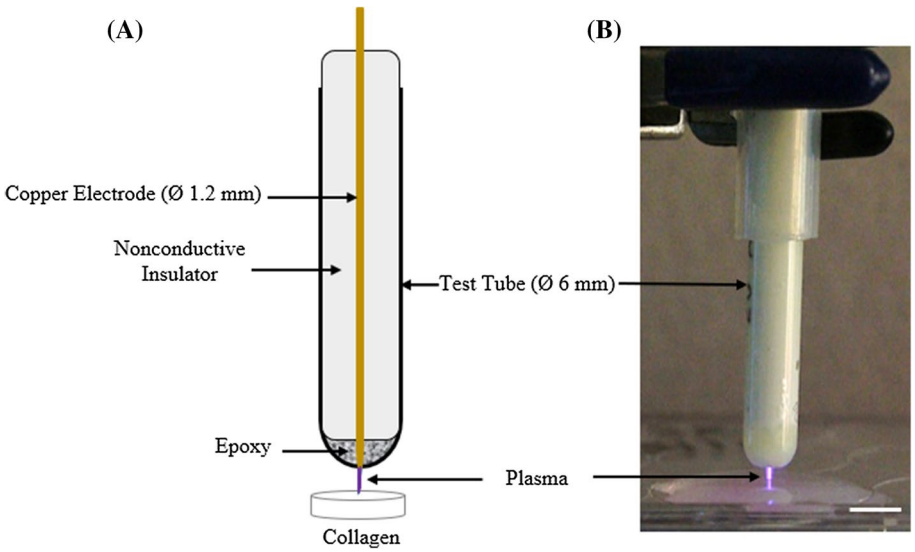

Fig. 1 **a** Schematic diagram of the non-thermal plasma system. **b** Photographic image of the non-thermal plasma system. Scale bar is 6 mm

separately in 12 well plates and in two different culture media recommended by ATCC. A549 lung cancer cells were cultured in Kaighn's modification of Ham's F-12 media (F-12K media; ATCC) and MRC-5 cells were cultured in Eagle's Minimum Essential Medium (EMEM; ATCC) supplemented with 10% fetal bovine serum (FBS; ATCC) at 37 °C with 5% CO_2 and humidity. Upon confluence, cells were trypsinized and suspended with media in 15 ml test-tube. For monolayer cell culture, A549 cells and MRC-5 cells were plated into the 12 well plate one day prior to plasma treatment. For A549 and MRC-5 cells, 1.5×10^{-5} and 2.0×10^{-5} cells were plated in each 12 well plate respectively and kept in an incubator overnight.

To generate cell encapsulated 3D collagen matrices, 2.5 mg/ml rat tail collagen type 1 (Advanced Biomatrix, USA) at pH range of 3–4 was neutralized using ice cold 1 N NaOH, 10× phosphate buffered saline (PBS) and deionized water based on our established protocol [3]. Cells at a density of 1.0×10^{-6} cells/ml for both cell line separately were mixed with neutralized collagen solution to create the 3D cell-encapsulated collagen matrix (CECM). 400 µl of CECM was then deposited to a well plate. The cell encapsulated collagen solution was further incubated for 15–20 min at 37 °C to get ~ 2 mm thick polymerized constructs. Then the media was added to each well plate which was further kept overnight in an incubator. On the following day, media was removed, and non-thermal plasma was applied directly to the CECM for 0 (control), 15, 30, 60, and 120 s.

Cell Viability

Cell viability was assessed using the live/dead cell assay (Life Technologies) consisting of Calcein-AM and Ethidium homodimer-1 (Eth-1). Cells-encapsulated collagen matrix (CECM) of ~ 2 mm thickness was treated with plasma for 15, 30, 60 and 120 s respectively. The Calcein-AM dye enters the live cells and is converted to Calcein by esterase that produces an intense green signal. On the other hand, Eth-1 will cross the membrane of the dead cells only and bind to the nucleic acids. A working solution was prepared by adding Eth-1 (2 µl) and Calcein AM (8 µl) to PBS (10 ml). Following plasma treatment, the cell-embedded collagen constructs were incubated with live/dead cells for 30 min in the dark. Confocal imaging of collagen was then performed immediately after plasma treatment and 24-h post-treatment to observe live and dead cells within the CECM at a different optical section. Images were acquired using the multi-photon laser scanning confocal microscope (Leica TCS SP5). For 3D reconstruction, Z stack images were captured using 15 µm optical sections and analyzed using MetaMorph imaging software.

Cell Cycle Analysis

The effect of plasma treatment on cell cycle is evaluated using flowcytometry. Following the plasma treatment, the percentage of cells in Sub-G1, G1, S and G2/M phases were evaluated at 24-h (day 1) and 48-h (day 2) after plasma treatment. Briefly A549 and MRC-5 cells embedded within collagen construct were treated with plasma for 15, 30, 60 and 120 s respectively and incubated for 24 and 48 h at 37 °C and 5% CO_2. Following incubation, cells were taken out using collagenase and collected using centrifugation which was then fixed with 1 ml cold 70% ethanol for 30 min at 4 °C. After fixation, cells were washed with phosphate buffered saline (PBS) and 50 µl of a 100 µg/ml of RNase (Life Technology) was added to digest RNA. Cells were then stained with 100 µl of Propidium Iodide (PI) (Life Technology) for 15 min at room temperature in the dark and were evaluated using FACS

Calibur flow cytometer (BD Bioscience, USA) and analyzed with Modfit LT 3.4 software for cell cycle.

Real-Time Quantitative PCR Analysis

Apoptosis specific gene expression was assessed using reverse transcription quantitative polymerase chain reaction (RT-qPCR) immediately after plasma treatment (day 0) and after 24-h incubation (day 1). A549 cancer and MRC-5 normal cells embedded within 3D collagen matrix were treated with plasma for 15, 30, 60 and 120 s respectively. Total RNA was isolated using the total RNA extraction kit (RNeasy mini kit; Qiagen). The RNA was then converted to cDNA using cDNA Reverse Transcription Kit (OMNISCRIPT kit; Qiagen). H2AX, p53, Caspase-8, ATM, and Bax gene expression analysis were performed using the Q BIORAD Real-Time PCR System (The Applied Biosystems, USA). 18s-RNA was used as a housekeeping gene. The primers sequences from published articles were purchased from the Integrated DNA Technologies (IDTs) (Table 1) [20, 21]. Relative quantification of gene expression was performed using the comparative threshold (C_T) method according to the $2^{-\Delta\Delta CT}$ method as described by the manufacturer. The C_T values of target genes (H2AX, p53, Caspase-8, ATM, and Bax) in each sample set (ΔC_T test sample) were normalized to those of 18sRNA. The $\Delta\Delta C_T$ was calculated by the formula $\Delta\Delta C_T = \Delta CT$ test sample $- \Delta C_T$ control. $\Delta\Delta C_T$ was converted to fold changes in mRNA gene expression relative to control by the equation $2^{-\Delta\Delta CT}$ [22]. The fold changes are presented as the mean ± SD. The primer sequences are shown in Table 1.

Extracellular Reactive Species Generation Upon Plasma Treatment

A monolayer A549 lung cancer cells and MRC-5 lung fibroblast cells were treated with plasma for 15, and 120 s. Immediately after treatment (day 0) and 24 h later (day 1), the plasma induced generation of hydrogen peroxide (H_2O_2) in media was measured using the Amplex Red Hydrogen Peroxide/Peroxidase Assay Kit (Invitrogen, USA). In the presence of horseradish peroxidase (HRP), the Amplex Red reagent reacts with hydrogen peroxide (H_2O_2) and produce the red fluorescent oxidation product known as resorufin [11]. A working solution of Amplex Red reagent (10-acetyl-3,7-dihydroxyphenoxazine) of 100 µM and HRP of 0.2 U/ml was prepared by mixing 50 µl of 10 mM Amplex Red, 100 µl of 10 U/ml HRP and 4.85 ml of 1X reaction buffer. Briefly, A549 cells and MRC-5 cells covered with 1 mm (360 µl) thick media and treated with plasma for 15 and 120 s. After treatment, 100 µl of media from plasma treated constructs and 100 µl

Table 1 Primer sequences used for the evaluation of the mRNA expression on A549 and MRC-5 cells [20, 21]

Genes	Forward primer [5′–3′]	Reverse primer [5′–3′]
18s rRNA	GAGTGTAAGGACCCATCGGA	CCTCCAATGGATCCTCGTTA
H2AX	TGGAAAGGGTCAGGGAAC G	GACTTGTGCTGGTATCTGGGT G
p53	TTACTCCCTCCATCTCCACC	TCATCAAACCCTTCAGCCAG
ATM	GGGCAACATGGTGAAACTCT	CCTTAACCTCCAGGGCTCAG
Caspase-8	TTGAACCCAAGAGGTCAAGG	ACGGGGTCTTGTTCTGTCAC
Bax	AACATGGAGCTGCAGAGGAT	CAGTTGAAGTTGCCGTCAGA

of working solution were mixed and analyzed by spectrophotometer (SpectraMax, USA) to measure the absorbance at 540 nm.

The Griess Assay (Cayman Chemical, USA) was used to measure the plasma-induced RNS generation at the extracellular space immediately after plasma treatment (day 0) and 24 h later (day 1). Addition of the Griess reagents converts the nitrite into a deep purple azo compound [23]. Briefly, after cells were exposed to the plasma in 12 well plates, 80 µl of treated media was transferred to the 96 well plate and mixed with 10 µl of cofactor and enzyme and incubated in the dark at room temperature for 1 h. Then, 50 µl of Griess assay reagent 1 (Sulphanilic Acid) and 50 µl of Griess assay reagent 2 (N-alpha-naphthyl-ethylenediamine) were added to the media and incubated for 10 min at room temperature to measure nitrite NO_2, the stable metabolite of NO, secreted to the culture medium. The absorbance was measured at 545 nm with a spectrophotometer (SpectraMax, USA) upon treatment.

Penetration of ROS and RNS Into Intracellular Space Upon Plasma Treatment

To quantitate intracellular generation of reactive oxygen and nitrogen species, A549 and MRC-5 cells plated in 12 well plate were exposed to plasma for 15 and 120 s. Reactive oxygen species (ROS) levels were assessed immediately after plasma treatment using the 2′,7′-dichlorodihydrofluorescein diacetate (H2DCFDA) (Life Technology) according to the manufacturer's protocol. After plasma treatment, both cells were washed with PBS and incubated with cell permeable 5 µM H2DCFDA for 30 min. H2DCFDA is oxidized by an intracellular generation of oxygen species and emits a bright green fluorescence. Florescence intensity was measured by a microplate reader (Bio-Rad, Hercules, CA) at 485/540 nm according to the manufacture's protocol. Relative value of ROS was calculated in terms of arbitrary fluorescence unit.

Similarly, intracellular reactive nitrogen species (RNS) were detected using the diaminofluorescein (DAF-2DA) (Cayman Chemicals). Following plasma treatment, cells were washed with PBS and incubated with 10 µM DAF-2DA for 30 min. DAF-2DA is a cell-permeable fluorescent nitric oxide (NO) indicator [23]. It is deacetylated by intracellular esterases and converted into DAF-2, that reacts with NO and yields the highly fluorescent triazofluorescein (DAF-2T) which was visualized using the fluorescence microscope (Cytation5, USA) at 490/525 nm excitation/emission. Untreated cells were used as a control to measure the basal intracellular NO level within A549 and MRC-5 cells. For the negative control, sodium pyruvate (10 mM) was used as an oxygen scavenger and 2-(4-carboxyphenyl)-4,4,5,5-tetramethylimidazoline-1-oxyl-3-oxid (cPTIO) (40 µM) was used as a nitrogen scavenger. Prior to plasma treatment, scavenger was added to the cells for 30 min and then visualized using the fluorescence microscope.

Statistical Analysis

Triplicate samples were used for the experimental and control groups. All statistical differences were determined using the student t test ($p < 0.05$). All values are reported as the mean and the standard deviation of the mean.

Results

Effect of Plasma on Cell Viability

Live/dead assays were conducted to study the viability of lung cancer and normal lung cells embedded within collagen matrix in response to non-thermal plasma treatment. Figure 2 shows the fluorescence images of live (green) and dead cells (red) captured with the confocal microscope following 0, 15, 30, 60 and 120 s plasma treatments. In control (0 s plasma treatment) of A549 and MRC-5 cells, all cells appeared green, indicating that all cells are live. In MRC-5, there were no dead cells for 15 s treated samples at day 0 and 1 post-treatment. For 30 s treated samples at day 0, there were no dead cells, but dead cells appeared 24 h post-treatment. As treatment time increases from 60 to 120 s, more dead cells appeared at the plasma treated area at day 0 and 1 post-treatment relative to 15 and 30 s (Fig. 2a). In day 0, the dead cells area for 120 s treated cells was 16.6 mm^2. On day 1, the dead cells area for 30, 60 and 120 s treatment time was 2.3 mm^2, 14.8 mm^2, and 24.8 mm^2, respectively (Fig. 2c).

Furthermore, in A549 lung cancer cells, dead cells start to appear even with lowest treatment time (15 s) at the plasma treated region (Fig. 2b). On day 0 post-treatment, the dead cells area increases from 0.85 to 28.89 mm^2 as the treatment time is increased from 15 to 120 s. On day 1 post-treatment, the dead cells area increases from 1.6 to 52.78 mm^2. These results demonstrated that on increasing the treatment time from 15 to 120 s, increases the number of dead cells and area. All the samples after 24-h post-treatment showed more dead cells than immediately after plasma treatment (day 0) due to the delayed effect of the plasma. The highest treatment time (120 s) had significant number of dead cells at both day 0 and 1 post-treatment (Fig. 2).

These results further suggest that the effect of plasma on the viability of cancer cells is higher than the normal cells.

Changes in Cell Cycle Following to Non-thermal Plasma Treatment

To study the effect of plasma on cell cycle progression of A549 and MRC-5 cells, we measured the percentage of cells in three distinct phases of cell cycle (G0/G1, S, and G2/M) by measuring the DNA content using Propidium Iodide (PI). The cell cycle analysis was done 24 h (day 1) and 48 h (day 2) after plasma treatment. At day 1, for 0 s plasma treatment (control) in A549 cells, 62% of cells were in G0/G1 phase, 18% cells in S-phase and 8% cells in G2/M phase (Fig. 3). For 15 and 30 s plasma treatment, we observed an increase in the percentage of cells in S-phase compared to control. The sample treated with 60 and 120 s showed a greater percentage of cells arrested in G2/M phase i.e. 17% and 26% respectively. The cells percentage in G2/M was increased by almost threefold compared to control for 120 s treatment time. The increase in the percentage of cells in S and G2/M phase is accompanied by decreases in G0/G1 phase (Fig. 3).

On day 1, In MRC-5 cells, for 0 s plasma treatment (control), G0/G1 had 50% of cells, S-phase had 22%, and G2/M phase had 9% (Fig. 3). In MRC-5 cells, the percentage of cells in all three phases were almost similar for all plasma treatment time.

Similarly, for A549 cells, after 48 h (day 2) of plasma treatment, ~ 19% of cells were in S phase and 28% of cells were in G2/M phase for 120 s sample (Fig. 4). This percentage is slightly higher than the percentage of cells in day 1 for 120 s plasma treated sample. After

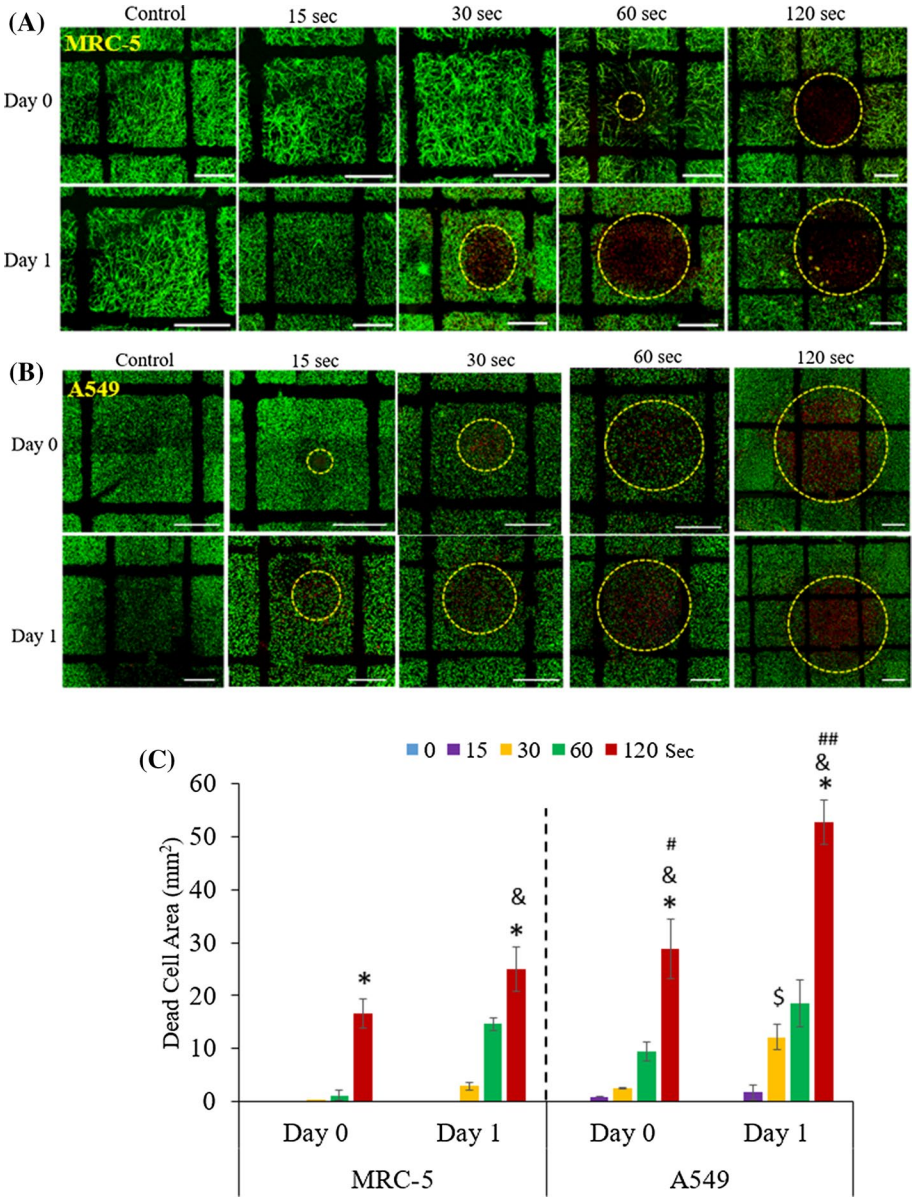

Fig. 2 **a** Fluorescence images of live (green) and dead (red) MRC-5 cells for 0 s (control), 15, 30, 60 and 120 s plasma treated samples. **b** Dead cell area increases on increasing treatment time on day 0 and 1 post-treatment. & and * denote statistical difference between 15, 60 and 120 s plasma treatment groups in day 0 and 1 post-treatment time for both MRC-5 and A549 cells, respectively ($p < 0.01$). # denote statistical difference between MRC-5 and A549 at day 0 post-treatment for 120-s ($p < 0.01$). ## denote statistical difference between MRC-5 and A549 for 120 s at day 1 post-treatment ($p < 0.01$). The yellow dotted circle was drawn to indicate the approximate diameter of the plasma-affected area containing dead cells. Scale bar is 500 μm; all images are × 10 and merged images (Color figure online)

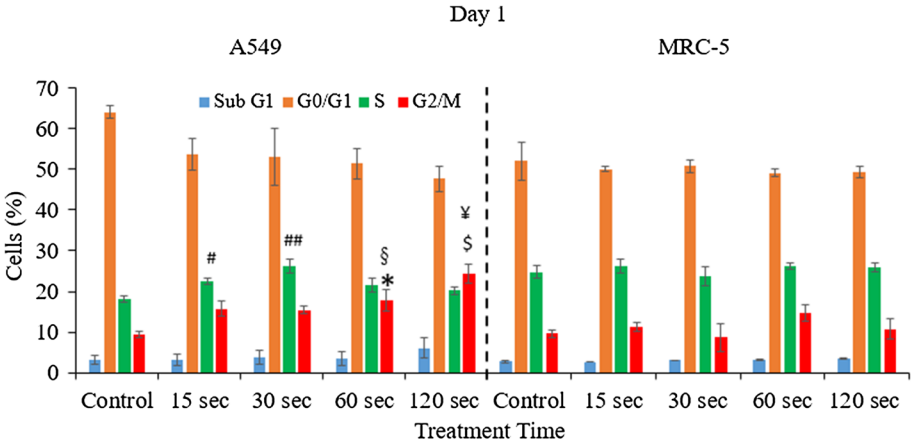

Fig. 3 A549 and MRC-5 cell distribution in different phases of cell cycle after plasma treatment with 24 h of incubation (day 1). Data are expressed as means ± SD (n = 3). #, ##, denote significant difference for S-phase between control and 15 and 30 s for A549 ($p < 0.05$). *, and $ denote significant difference for G2/M phase between control and 60, and control and 120 s for A549 ($p < 0.02$). § and §§ denote significant difference in G2/M phase of 60 and 120 s between A549 and MRC-5 cells ($p < 0.05$)

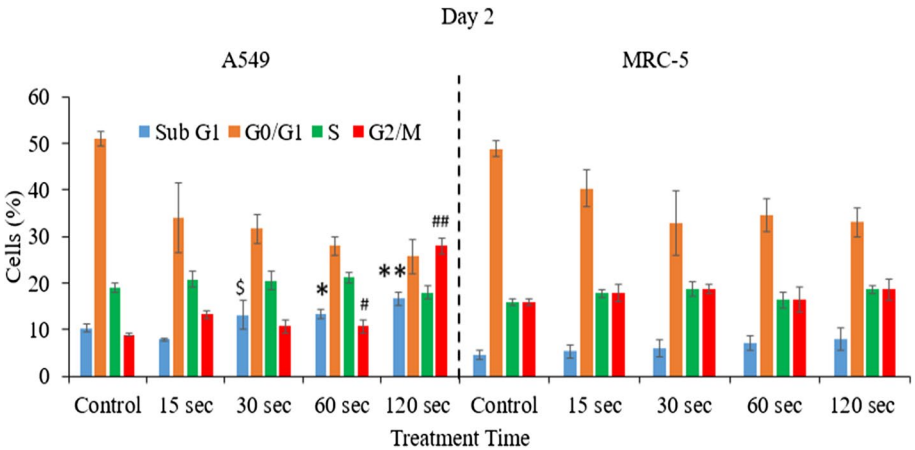

Fig. 4 A549 and MRC-5 cell distribution in different phases of cell cycle after 48 h of incubation (day 2). Data are expressed as means ± SD (n = 3). $, *, and **, denote significant difference for Sub-G1 phase between control and 30, 60 and 120 s for A549 cells ($p < 0.05$). #, ##, denote significant difference between control and 60 and 120 s for G2/M phase for A549 cells ($p < 0.05$)

48 h of plasma treatment, we observed gradual increases in percentage of cells in Sub-G1 (apoptotic phase) from 15 to 120 s samples. However, in MRC-5, after 48 h of plasma treatment, we observed a little increase in percentage of cells in G2/M phase compared to control. And for 120 s treatment time, the cells percentage were similar in S and G2/M phase (~ 17%) (Fig. 4).

These results demonstrated that in cancer cells, plasma arrested the cell cycle at S phase for lower treatment times (15 and 30 s) whereas for longer treatment times (60 and 120 s)

cells were arrested in G2/M phase. These data also suggested that plasma had greater effect on cell cycle arrest of cancer cells at G2/M phase than on normal cells.

Non-thermal Plasma Induced Gene Expression

We analyzed the expression of apoptosis-related genes due to non-thermal plasma treatment on both A549 and MRC-5 cells. Apoptosis-related genes H2AX, p53, Caspase-8, ATM and BAX in A549 cells exposed to plasma for 15 s and 120 s were highly expressed at day 1 post-treatment. For 120 s plasma treated sample, there was up to 33.5-fold increase in p53 and BAX expression. H2AX was tenfold upregulated in A549 cells at day 1 post-treatment for 120 s sample (Fig. 5). ATM and Caspase-8 were less up-regulated in comparison to other genes. 15-s treated samples had enhanced BAX gene expression. ATM was sixfold upregulated at day 1 post-15 s treatment. Caspase-8, H2AX, and p53 were upregulated to a lesser extent than BAX and ATM in 15 s treated samples (Fig. 5).

Unlike A549 cancer cells, MRC-5 normal cells did not show dramatic changes in apoptosis related gene expression. At day 1 post-treatment, H2AX gene expression showed a 3.6-fold up-regulation while p53, Caspase-8, ATM and BAX were expressed lower than H2AX for 120 s treated samples. Capase-8, p53, ATM, and BAX are 2.3, 2.4 and onefold expressed for 120 s sample (Fig. 5).

For A549 cells, at day 2 post-treatment, Caspase-8 and ATM was almost eightfold and 6.5-fold upregulated for 120 s treated samples respectively (Fig. 6). For 15 s treated samples, BAX was fourfold expressed. H2AX, p53, and BAX were less expressed than the Caspase-8 and ATM for both 120 and 15 s treated samples. In compare to day 1 and day 2 post-treatment, all genes were expressed to a greater extent on day 1 post-treatment than day 2 post-treatment for both 15 and 120 s treated samples.

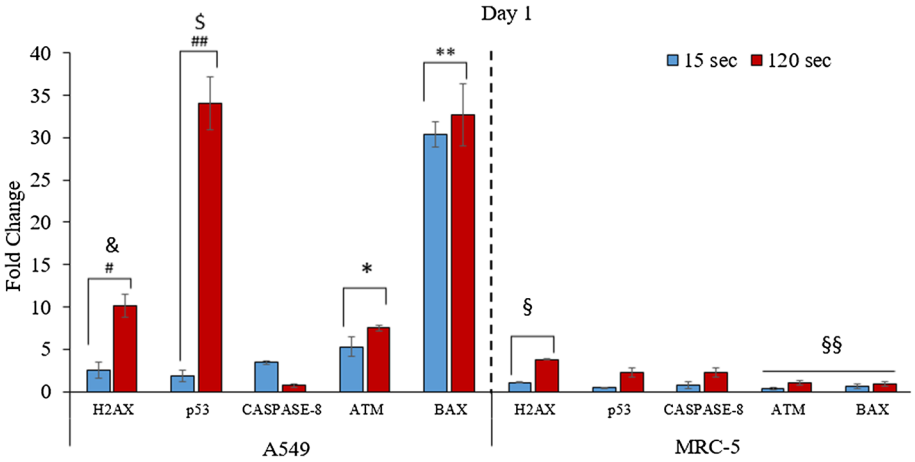

Fig. 5 Expression of apoptosis-related genes induced by the non-thermal plasma in A549 and MRC-5 cells at day 1 post-treatment. Data are expressed as means ± SD (n = 3). # and ## denote significantly significant differences between 15 and 120 s for H2AX and p53 for A549 ($p < 0.001$). * and ** denote significant difference between 15 and 120 s for ATM and BAX for A549 ($p < 0.05$). &, $ and §§ denote significant difference between A549 and MRC-5 for H2AX, p53, ATM and BAX, respectively, ($p < 0.001$). § ($p < 0.002$) when comparing H2AX in-between 15 and 120 s for MRC-5

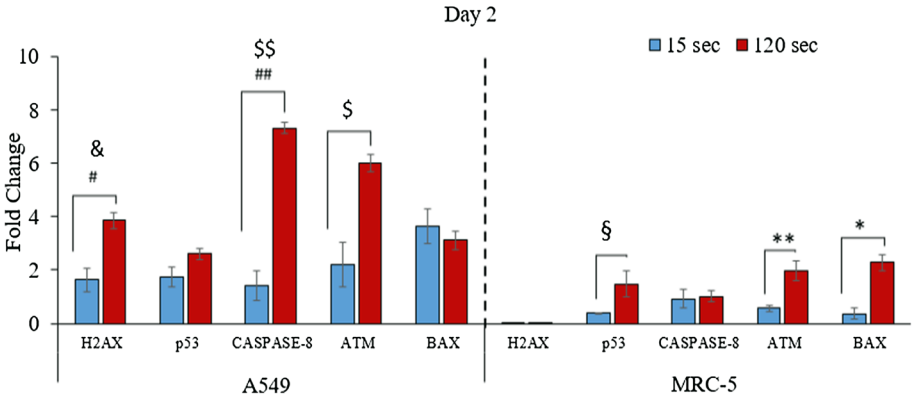

Fig. 6 Expression of apoptosis-related genes induced by the non-thermal plasma in A549 and MRC-5 cells at day 2 post treatment. Data are expressed as means ± SD (n = 3). #, ##, and $ denote significant difference between 15 and 120 s for H2AX, caspase-8 and ATM for A549 respectively, ($p < 0.001$). & and $$ denote significant difference for H2AX and caspase-8 between A549 and MRC-5 ($p < 0.001$). §, * and ** denote significant difference between 15 and 120 s for p53, BAX and ATM in MRC-5

Similarly, for MRC-5 cells, at day 2 post-treatment, there was a higher expression of BAX, ATM, and p53 relative to day 1. BAX was expressed 2.3-fold whereas ATM was expressed twofold for 120 s treated samples. p53, Caspase-8, ATM and BAX gene expression were less for 15 s sample than the 120 s treated sample (Fig. 6).

Reactive Species at Extracellular Space

We further investigated the generation of reactive species within media upon plasma treatment. Following 15 and 120 s non-thermal plasma treatment, the extracellular production of oxygen species and nitrogen species in the culture media of both normal lung (MRC-5) and cancer cells (A549) were measured using the Amplex Red and Griess Assay, respectively.

In A549 cells, at day 0, immediately after 120 s treatment time, the extracellular generation of H_2O_2 was 26-fold higher than in the control sample. For 15 s treatment time, H_2O_2 increased only by fourfold at day 0 (Fig. 7a). This suggests that the generation of reactive oxygen species is dose-dependent. After 24 h, H_2O_2 reduced significantly relative to day 0 for 120 s and 15 s treated sample.

In order to measure the nitrogen species, nitrite (NO_2) was measured as a stable metabolite of nitric oxide (NO). Figure 7b showed the different concentration of NO_2 generated in A549 at day 0 and 1 upon plasma treatment, with respect to the treatment duration. In A549 at day 0, with 15 s treatment, there was a 5.2-fold increase in NO_2 amount within the culture media compared to the control (untreated cells). As the treatment time is increased to 120 s, there was a significant 22-fold rise in NO_2 compared to the control (untreated cells). The amount of nitrogen species within the media increases after prolonged treatment time. However, at day 1, the amount of nitrogen species was reduced to threefold and 12-fold for both 15 and 120 s plasma treated groups, respectively, compared to the control (untreated group). This reduction of reactive species at day 1 might be because of intracellular penetration of reactive species and conversion to other chemical compounds. The

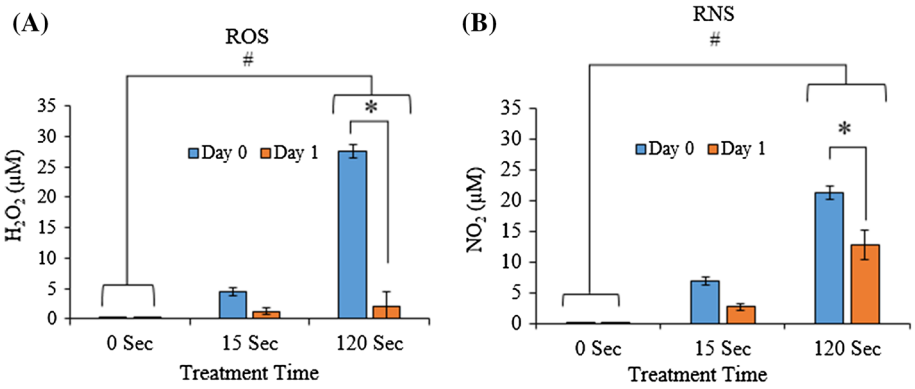

Fig. 7 Production of different concentration of reactive species within A549 cell culture media **a** H_2O_2, **b** NO_2. Results are expressed as mean ± SD of H_2O_2 and NO_2 concentration (μM) (n = 3). * denote statistically significant differences between day 0 and 1 for 120 s ($p < 0.001$). # denote statistically significant difference between control (0 s) and 120 s ($p < 0.001$)

extracellular production of ROS and RNS in MRC-5 cell was similar to the A549 cells and data are presented as the supplementary data.

Penetration of ROS and RNS into Intracellular Space

This experiment was done to measure the reactive oxygen and nitrogen species (RONS) penetrated intracellularly due to the plasma on both cancer and normal lung cells. The intracellular reactive oxygen species level was analyzed by measuring H2DCFDA that had penetrated into intracellular space. The control sample (untreated) of both cells did not develop fluorescent color because the cells were devoid of reactive oxygen species. After treating the cancer cell with plasma for 15 and 120 s, exogenous oxygen species get diffused into intracellular space and cells fluoresce green upon reaction with H2DCFDA assay. In A549 cells, results showed that for higher treatment time (120 s) there was higher fluorescent intensity than the 15 s treated sample due to the higher plasma dose and increased treatment area (Fig. 8a). Similarly, intracellular nitrogen species for 15 and 120 s sample were measured using DAF-2DA assay. Both samples developed less green fluorescence than the ROS samples (Fig. 8c). This revealed that penetration of intracellular ROS was higher than the RNS in cancer cells.

In MRC-5, results showed that for longer treatment time (120 s) there was a higher fluorescent intensity of ROS and covers a larger area of green fluorescent than the 15 s treated sample due to a higher plasma dose (Fig. 9a). The fluorescent due to RNS was very diminishing compare to ROS (Fig. 9b).

In contrast to cancer cells, normal cells developed less bright green fluorescence due to ROS and showed a smaller area of green fluorescence for both 15 and 120 s (Fig. 9a). Use of a ROS and RNS scavenger as a negative control abolished the intracellular production of oxygen and nitrogen species due to plasma treatment and lacked formation of green fluorescent. In MRC-5 samples, the fluorescent intensity due to RONS for 15 and 120 s treatments was less compared to A549 samples.

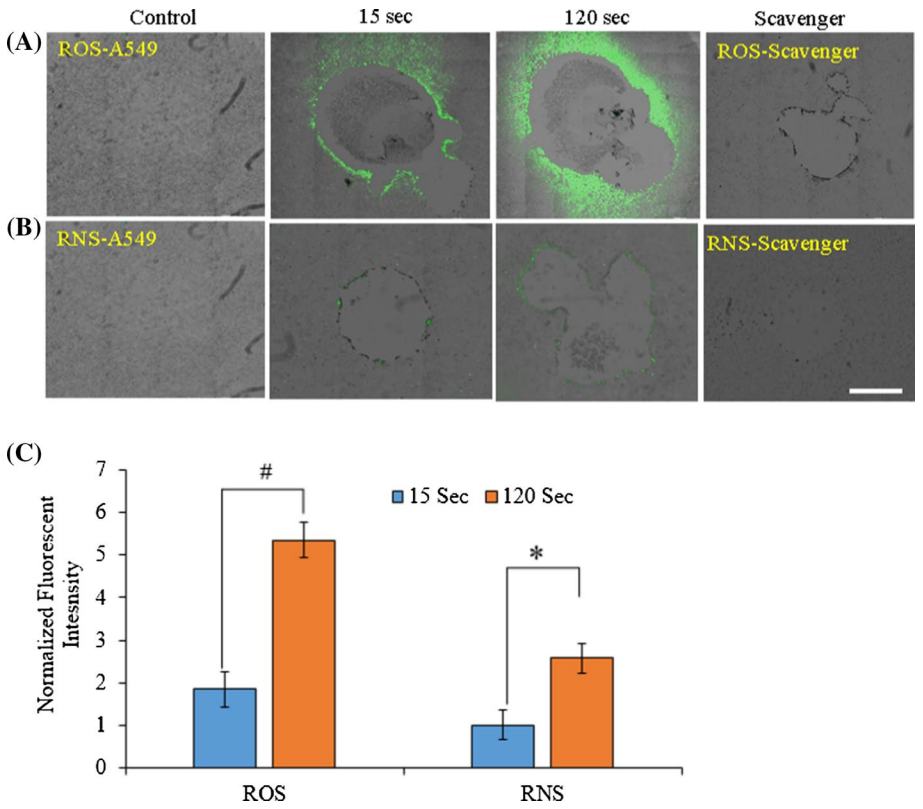

Fig. 8 Intracellular production of reactive species upon plasma treatment in A549 cells for 0 s (control), 15 s, 120 s and ROS or RNS scavenger **a** ROS, **b** RNS, **c** normalized fluorescence intensity of ROS and RNS produced for 15 and 120 s sample. #, * denote statistically significant differences between 15 and 120 s plasma treatment group for ROS and RNS respectively ($p < 0.05$). Scale bar is 2000 µm

These results suggested that the intracellular reactive oxygen species produce in response to plasma treatment are greater than reactive nitrogen species in cancer cells compared to normal lung cells. This may indicate that cancer cells are more susceptible to oxygen species than normal cells.

Discussion

The field of plasma medicine is rapidly advancing towards the development of new medical therapies [24, 25]. Plasma has been used for various applications such as surface modification treatment [26–28], dental cavities [29], bacterial sterilizations [30–33], cell detachment [18], and wound healing [34]. The promising results published by several group have demonstrated the potential of this technology for the cancer treatment [35, 36]. Plasma oncology research is a growing field where researcher could contribute a lot to answer so many of important questions that is still unanswered [36].

In this research study, we compared the effect of non-thermal plasma in between cancerous lung cells A549 and normal fibroblast lung cells MRC-5. Both cells lines are

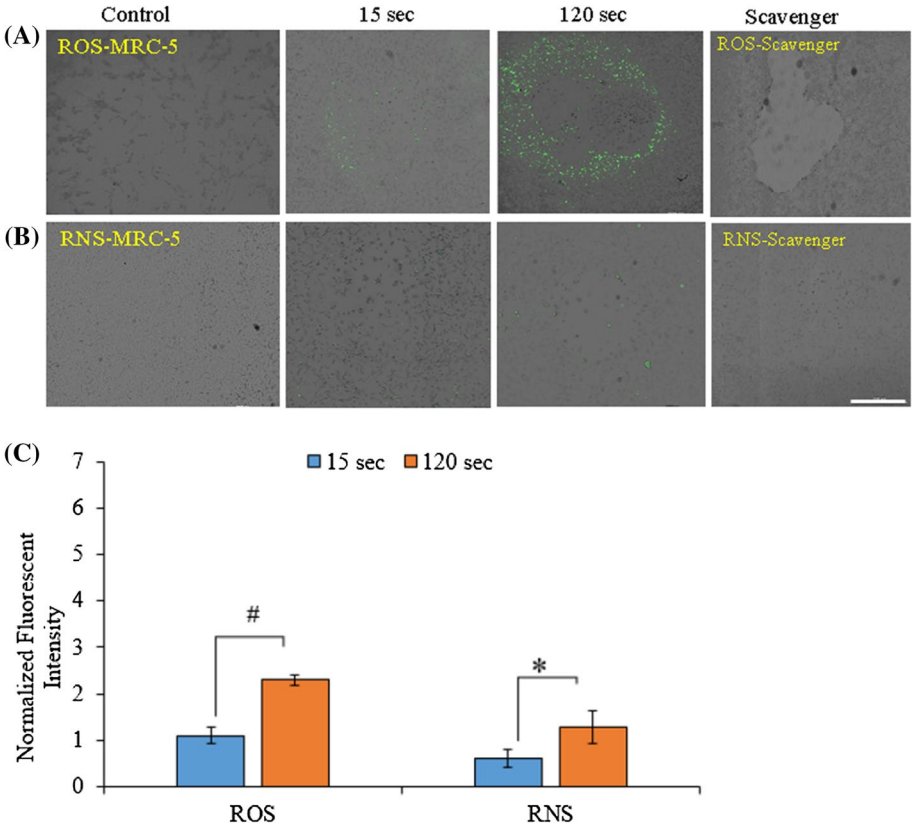

Fig. 9 Intracellular generation of reactive species on MRC-5 cells for control (untreated), 15 s, 120 s and ROS or RNS scavenger **a** ROS, **b** RNS, **c** normalized fluorescence intensity of ROS and RNS produced for 15 and 120 s treated samples. #, * denote statistically significant differences between 15 and 120 s plasma treatment group for ROS and RNS respectively ($p < 0.05$). Scale bar is 2000 µm

morphologically and functionally different and has shown different responses to plasma treatment. Our results showed significant loss of A549 lung cancer cells viability in compare to the MRC-5 normal lung fibroblast cells after plasma treatment which indicated its cytotoxic effect. In cancer cells, even with the shortest treatment time (15 s), cells tend to die, and cell death increases with increase in treatment time (Fig. 2). The uptake of oxygen species is higher in cancer cells in comparison to the normal cells which causes the intracellular oxidative stress to the cells. As treatment time increases, the plasma dose also increases, ultimately causing oxidative stress to more cells, leading to more cell death. Similar results were demonstrated by Kim et al. [5] group where they studied the cell viability of normal and carcinoma cells caused by plasma generated reactive species. In normal lung cells, dead cells were observed for 60 and 120 s at both day 0 and 1 treatment time. Although, plasma impacted cell viability in normal cells for higher treatment time, the dead cells area was greater for cancer cells in compare to the healthy cells (Fig. 2). Our result showed that the uptake of oxygen species by normal cells is less in compared to the cancer cells, causing less cell death in normal cells.

Moreover, we studied the effect of plasma on cell cycle. Plasma effects on cell cycle revealed that in A549 cells, after 24 h, more cells were arrested in G2/M phase for longer treatment time (120 s). Whereas, for shorter treatment times (15 and 30 s) a greater percentage of cells were observed in S-phase. After 48 h post-treatment, 120 s plasma treated samples showed an increased percentage of cells in G2/M phase along with significant number of cells in sub-G1 phase (Fig. 4). Kim et al. [37] studied the cell growth arrest in colorectal cancer cells due to plasma. They found increase in B-catenin phosphorylation in cells due to plasma leading to anti proliferative effect. Vandamme et al. [38] demonstrated significant fewer cells in G0/G1 phase but an increase in cells in S and G2/M phases due to cell cycle arrest. This may be because of formation of DNA strand break and induction of apoptotic cell death signaling pathways in response to plasma. This cell cycle arresting effect of plasma was possibly due to decreased metabolic activity (e.g., cellular repair mechanisms) affecting the cell division rate triggered due to intracellular stress. Plasma-induced double-stranded DNA damage causing cell cycle checkpoint arrest is through phosphorylation of p53 in order to activate apoptosis [39]. This cell cycle arresting effect is significantly higher in cancer cells relative to normal cells [20, 22].

In addition to the cell cycle arresting effect of the plasma, we examined the expression of genes involved in apoptosis. We assessed H2AX, BAX, p53, ATM, and Caspase-8 to investigate a potential mechanism by which non-thermal plasma may induce apoptosis in cancer cells. We evaluated whether plasma could induce DNA damage by examining phosphorylation of H2AX [12, 40]. H2AX is a histone variant that is phosphorylated in response to DNA damage, forming γ-H2AX. Phosphorylation of H2AX was commonly observed in numerous plasma-treated cells and it was more significantly expressed in cancer cells than in normal cells [41]. Intracellular reactive species causes stress and DNA damage because deoxyribose sugar moieties and nucleobases of DNA are susceptible to their direct attack. This observation indicates that plasma exposure selectively induces DNA damage that leads to A549 cell apoptosis. Kim et al. [42] demonstrated DNA damage and mitochondria dysfunction induced by plasma leading to cell apoptosis. Similarly, Kaushik et al. [43] studied the apoptotic response caused in human monocytic lymphoma cells due to plasma.

We then evaluated expression of BAX, p53, ATM, and Caspase-8, apoptosis-related mRNA. BAX is involved in mitochondria membrane signaling in the process of early apoptosis [20]. Phosphoprotein p53 is a tumor suppressor gene which regulates apoptosis of a cell and prevents tumor progression [44, 45]. Ataxia-telangiectasia mutated (ATM) is a large protein kinase family which is recruited and activated by double-strand DNA breaks. It phosphorylates several key proteins including H2AX and p53 that initiate the activation of the DNA damage checkpoint leading to cell cycle arrest and apoptosis [46, 47]. Caspase-8 is a part of a family of caspases, aspartate-specific cysteine proteases, which activate apoptosis signaling of a cell and can also activate pro-apoptotic Bcl-2 family members [39].

We studied the apoptotic gene expression due to plasma in between cancerous A549 lung cells and normal MRC5 fibroblast lung cells grown in two separate culture media. Our results showed that plasma significantly increase expression of all pro-apoptotic genes. The higher expression of pro-apoptotic genes in A549 cancer cells in compare to MRC-5 normal cells is probably due to the genetical and morphological difference in between those two cells. Lung cancer cells exposed to plasma for 15 and 120 s showed higher expression of BAX. Higher BAX gene expression results in mitochondrial membrane potential (MMP) attenuation, which ultimately activates mitochondrial mediated apoptosis [11, 48]. There was also significantly higher expression of p53 gene expression for 120 s treated

sample relative to 15 s treated samples and slightly enhanced expression of H2AX and ATM at day 1 post-treatment. When cells are subjected to the cellular stress, p53 is activated, that regulates cell cycle arrest and apoptosis by affecting the expression of its target genes, including cyclin-dependent kinase (CDK) inhibitors and cell death genes BAX, and FAS [49]. Previous reports have demonstrated the higher expression of apoptosis-related genes. This significant level of increased gene expression indicates the induction of apoptosis in cancer cells. The level of expression of genes was less in day 2 post-treatment cells compared to day 1 post-treatment cancer cells.

Induction of apoptosis is an effective way to halt tumor growth. Fridman et al. showed the apoptotic behavior of plasma in melanoma and skin cancer cells. Plasma generated RONS activated apoptosis triggers expression of different pro-apoptotic genes. Mitochondria are primarily affected due to RONS in the early apoptotic process and are now thought to act as the central coordinators of cell death. The plasma generated reactive species can activate the mitochondrial intrinsic apoptosis pathway by changing in Mitochondrial Membrane Potential (MMP). Change in MMP cause the upregulation of BAX gene along with the release of Cytochrome C (Cyt C) that activates the caspase pathway and eventually cell undergoes apoptosis. In addition, RONS causes the upregulation of Caspase-8 and due to the DNA breakage; H2AX mRNA gene expression levels also increase in response to RONS. On the other hand, ATM and p53 are upregulated and cause the apoptosis of cancer cells.

Moreover, in normal MRC-5 lung cells, H2AX, p53, Caspase8, ATM, and BAX were all less upregulated compared to cancer cells in response to plasma. In A549 cells, all genes were upregulated by more than eightfold except for Caspase-8 at day 1 post-treatment (Fig. 5). The level of gene expression at day 2 post-treatment was reduced relative to day 1 post-treatment for the normal cells. These results demonstrated that apoptosis-related genes were upregulated in cancer cells to a greater extent than in normal cells with response to plasma. These result further suggested that non-thermal plasma destroyed the intracellular structures, DNA, and mitochondria of cancer cells, inducing apoptosis [20]. In addition, the DNA or mitochondria damage is probably due to the accumulation of intracellular reactive species in cancer cells that cause mitochondrial dysfunction and endoplasmic reticulum-stress [20, 50].

Non-thermal plasma generates different reactive species such as reactive oxygen species (ROS), reactive nitrogen species (RNS) [51]. As mentioned above these species have critical roles in reducing the viability of cancer cells, and inducing apoptosis [18, 39]. Similar studies were reported by Yan et al. [52] in principles of using cold atmospheric plasma stimulated media for cancer treatment. Kim et al. [53] studied the production of several intracellular reactive oxygen species that causes reduction in in cell viability. Another study by Utsumi et al. [54] demonstrated the effect of indirect non-equilibrium atmospheric pressure plasma on anti-proliferation of chemo-resistant ovarian cancer cells in vitro and in vivo. Also, Bauer et al. [55] studied the selective anticancer mechanisms of the reactive oxygen and nitrogen species.

Reactive species generated by the plasma diffuses in the media covering cells and finally enters the cells. Extracellular reactive species enter the intracellular space of cells through the transmembrane diffusion process. Aquaporins (AQPs), a specific water channel, facilitate the diffusion of H_2O_2. Within the AQPs family, AQP 1,3,8 and 9 are believed to play important role in the anticancer capacity of plasma, particularly in terms of transmembrane diffusion of the plasma originated H_2O_2 [52]. Our results showed that extracellular generation of RONS was almost the same for both cancer and normal cells. However, intracellular generation of RONS was higher for cancer cells than the normal cells (Figs. 8 and 9). This

difference in rising ROS levels in the normal and cancerous cells is due to the difference in basal intracellular ROS level. It is thought that the stronger metabolism in cancerous cells influences elevated ROS basal level relative to the normal cells. When additional ROS enters the cancer cells, the whole intracellular stress due to ROS passes a threshold more easily than the normal cells [23]. The amount of generation of reactive species is directly proportional to the treatment time. As treatment time increases, the production of reactive species also increases, which subsequently increases the intracellular stress to the cancer cells. The exerted intracellular stress due to the reactive species to the cancer cells induces the mitochondrial dysfunction [10, 50]. These difference in generation of intracellular oxidative stress has different effect of plasma on cell viability and apoptosis in between normal and cancer cells. Due to the difference in morphology and function of lung cancer and normal lung cells, the uptake of oxygen generated by plasma is different, resulting in difference in oxidative stress, which ultimately cause difference in cell viability and cell cycle. In addition to that, due to the genetical difference in between normal cells and cancer cells the pre-apoptotic gene expression in cancer cells was higher than normal cells resulting in apoptosis of cancer cells due to plasma.

Conclusion

In conclusion, differential effect of plasma was studied separately in between lung cancer cells (A549) and normal lung cells (MRC-5) and our results demonstrated that intracellular penetration of RONS was greater in cancer cells than in normal cells. The intracellular generation of reactive species was dose-dependent in response to plasma treatment. In addition, plasma treatment in cancer cells arrested the cell cycle at the G2/M phase at 24-h post-treatment. Furthermore, we demonstrated the higher expression of apoptosis-related genes in cancer cells in compare to normal healthy cells in response to the plasma treatment. Our results that were obtained by treating lung cancer cells (A549) and normal lung fibroblast cells (MRC-5) with plasma, suggest that dielectric barrier discharge non-thermal plasma produced RONS that induces cell cycle arrest and damages the intracellular DNA or mitochondria, which ultimately induce apoptosis in cancer cells, relative to normal cells.

References

1. Molina JR, Yang P, Cassivi SD, Schild SE, Adjei AA (2008) Non-small cell lung cancer: epidemiology, risk factors, treatment, and survivorship. Mayo Clin Proc 83:584–594
2. American Lung Association-Lung Cancer Fact Sheet 2016. http://www.lung.org
3. Karki S, Thapa Gupta T, Yildirim-Ayan E, Eisenmann K, Ayan H (2017) Investigation of non-thermal plasma effects on lung cancer cells within 3D collagen matrices. J Phys D Appl Phys 50:315401
4. Keidar M, Walk R, Shashurin A, Srinivasan P, Sandler A et al (2011) Cold plasma selectivity and the possibility of a paradigm shift in cancer therapy. Br J Cancer 105:1295–1301
5. Kim SJ, Chung TH (2016) Cold atmospheric plasma jet-generated RONS and their selective effects on normal and carcinoma cells. Sci Rep 6:20332
6. Ghimire B, Sornsakdanuphap J, Hong YJ, Uhm HS, Weltmann K-D et al (2017) The effect of the gap distance between an atmospheric-pressure plasma jet nozzle and liquid surface on OH and N_2 species concentrations. Phys Plasmas 24:073502
7. Ghimire B, Subedi DP, Khanal R (2017) Improvement of wettability and absorbancy of textile using atmospheric pressure dielectric barrier discharge. AIP Adv 7:085213
8. Ayan H, Yildirim ED, Pappas DD, Sun W (2011) Development of a cold atmospheric pressure microplasma jet for freeform cell printing. Appl Phys Lett 99:111502

9. Ayan H, Fridman G, Gutsol AF, Vasilets VN, Fridman A et al (2008) Nanosecond-pulsed uniform dielectric-barrier discharge. IEEE Trans Plasma Sci 36:504–508
10. Ahn HJ, Kim KI, Hoan NN, Kim CH, Moon E et al (2014) Targeting cancer cells with reactive oxygen and nitrogen species generated by atmospheric-pressure air plasma. PLoS ONE 9:e86173
11. Kaushik N, Uddin N, Sim GB, Hong YJ, Baik KY et al (2015) Responses of solid tumor cells in DMEM to reactive oxygen species generated by non-thermal plasma and chemically induced ROS systems. Sci Rep 5:8587
12. Kalghatgi S, Kelly CM, Cerchar E, Torabi B, Alekseev O et al (2011) Effects of non-thermal plasma on mammalian cells. PLoS ONE 6:e16270
13. Blackert S, Haertel B, Wende K, von Woedtke T, Lindequist U (2013) Influence of non-thermal atmospheric pressure plasma on cellular structures and processes in human keratinocytes (HaCaT). J Dermatol Sci 70:173–181
14. Hirst AM, Simms MS, Mann VM, Maitland NJ, O'Connell D et al (2015) Low-temperature plasma treatment induces DNA damage leading to necrotic cell death in primary prostate epithelial cells. Br J Cancer 112:1536–1545
15. Kwon BS, Choi EH, Chang B, Choi JH, Kim KS et al (2016) Selective cytotoxic effect of non-thermal micro-DBD plasma. Phys Biol 13:056001
16. Liedtke KR, Bekeschus S, Kaeding A, Hackbarth C, Kuehn J-P et al (2017) Non-thermal plasma-treated solution demonstrates antitumor activity against pancreatic cancer cells in vitro and in vivo. Sci Rep 7:8319
17. Nakamura K, Peng Y, Utsumi F, Tanaka H, Mizuno M et al (2017) Novel intraperitoneal treatment with non-thermal plasma-activated medium inhibits metastatic potential of ovarian cancer cells. Sci Rep 7:6085
18. Karki SB, Yildirim-Ayan E, Eisenmann KM, Ayan H (2017) Miniature dielectric barrier discharge nonthermal plasma induces apoptosis in lung cancer cells and inhibits cell migration. Biomed Res Int 2017:12
19. Georgescu N, Lupu AR (2010) Tumoral and normal cells treatment with high-voltage pulsed cold atmospheric plasma jets. IEEE Trans Plasma Sci 38:1949–1955
20. Panngom K, Baik KY, Ryu YH, Uhm HS, Choi EH (2013) Differential responses of cancer cell lines to non-thermal plasma from dielectric barrier discharge. Curr Appl Phys 13:S6–S11
21. Kumar N, Attri P, Yadav DK, Choi J, Choi EH et al (2014) Induced apoptosis in melanocytes cancer cell and oxidation in biomolecules through deuterium oxide generated from atmospheric pressure non-thermal plasma jet. Sci Rep 4:7589
22. Hansakul P, Aree K, Tanuchit S, Itharat A (2014) Growth arrest and apoptosis via caspase activation of dioscoreanone in human non-small-cell lung cancer A549 cells. BMC Complement Altern Med 14:413
23. Mostafa E, Gayathri S, Halim A, Eda Y-A (2015) Exogenous nitric oxide (NO) generated by NO-plasma treatment modulates osteoprogenitor cells early differentiation. J Phys D Appl Phys 48:345401
24. Stoffels E, Sakiyama Y, Graves DB (2008) Cold atmospheric plasma: charged species and their interactions with cells and tissues. IEEE Trans Plasma Sci 36:1441–1457
25. Ayan H, Fridman G, Staack D, Gutsol AF, Vasilets VN et al (2009) Heating effect of dielectric barrier discharges for direct medical treatment. IEEE Trans Plasma Sci 37:113–120
26. Chengyang W, Qudus H, Jessica S, Halim A, Wei S (2015) Localized surface functionalization of polycaprolactone with atmospheric-pressure microplasma jet. Biomed Phys Eng Express 1:025002
27. Yildirim ED, Ayan H, Vasilets VN, Fridman A, Guceri S et al (2008) Effect of dielectric barrier discharge plasma on the attachment and proliferation of osteoblasts cultured over poly(ε-caprolactone) scaffolds. Plasma Processes Polym 5:58–66
28. Ayan H, Staack D, Fridman G, Gutsol A, Mukhin Y et al (2009) Application of nanosecond-pulsed dielectric barrier discharge for biomedical treatment of topographically non-uniform surfaces. J Phys D Appl Phys 42:125202
29. Ranjan R, Krishnamraju PV, Shankar T, Gowd S (2017) Nonthermal plasma in dentistry: an update. J Int Soc Prev Community Dent 7:71–75
30. Sanaei N, Ayan H (2015) Bactericidal efficacy of dielectric barrier discharge plasma on methicillin-resistant *Staphylococcus aureus* and *Escherichia coli* in planktonic phase and colonies in vitro. Plasma Med 5:1–16
31. Gupta TT, Karki SB, Matson JS, Gehling DJ, Ayan H (2017) Sterilization of biofilm on a titanium surface using a combination of nonthermal plasma and chlorhexidine digluconate. Biomed Res Int 2017:11

32. Gupta TT, Matson JS, Ayan H (2018) Antimicrobial effectiveness of regular dielectric-barrier discharge (DBD) and jet DBD on the viability of *Pseudomonas aeruginosa*. IEEE Trans Radiat Plasma Med Sci 2:68–76
33. Gupta T, Karki S, Fournier R, Ayan H (2018) Mathematical modelling of the effects of plasma treatment on the diffusivity of biofilm. Appl Sci 8:1729
34. Kubinova S, Zaviskova K, Uherkova L, Zablotskii V, Churpita O et al (2017) Non-thermal air plasma promotes the healing of acute skin wounds in rats. Sci Rep 7:45183
35. Kieft IE, Dvinskikh NA, Broers JLV, Slaaf DW, Stoffels E (2004) Effect of plasma needle on cultured cells. SPIE
36. Kajiyama H, Utsumi F, Nakamura K, Tanaka H, Toyokuni S et al (2017) Future perspective of strategic non-thermal plasma therapy for cancer treatment. J Clin Biochem Nutr 60:33–38
37. Kim CH, Bahn JH, Lee SH, Kim GY, Jun SI et al (2010) Induction of cell growth arrest by atmospheric non-thermal plasma in colorectal cancer cells. J Biotechnol 150:530–538
38. Vandamme M, Robert E, Lerondel S, Sarron V, Ries D et al (2012) ROS implication in a new antitumor strategy based on non-thermal plasma. Int J Cancer 130:2185–2194
39. Schmidt A, Bekeschus S, von Woedtke T, Hasse S (2015) Cell migration and adhesion of a human melanoma cell line is decreased by cold plasma treatment. Clin Plasma Med 3:24–31
40. Volotskova O, Hawley TS, Stepp MA, Keidar M (2012) Targeting the cancer cell cycle by cold atmospheric plasma. Sci Rep 2:636
41. Kim SJ, Chung TH, Bae SH, Leem SH (2010) Induction of apoptosis in human breast cancer cells by a pulsed atmospheric pressure plasma jet. Appl Phys Lett 97:023702
42. Kim GJ, Kim W, Kim KT, Lee JK (2010) DNA damage and mitochondria dysfunction in cell apoptosis induced by nonthermal air plasma. Appl Phys Lett 96:021502
43. Kaushik N, Kumar N, Kim CH, Kaushik NK, Choi EH (2014) Dielectric barrier discharge plasma efficiently delivers an apoptotic response in human monocytic lymphoma. Plasma Process Polym 11:1175–1187
44. Kastan MB, Canman CE, Leonard CJ (1995) P53, cell cycle control and apoptosis: implications for cancer. Cancer Metastasis Rev 14:3–15
45. Chen F, Chang D, Goh M, Klibanov SA, Ljungman M (2000) Role of p53 in cell cycle regulation and apoptosis following exposure to proteasome inhibitors. Cell Growth Differ 11:239–246
46. Pellegata NS, Antoniono RJ, Redpath JL, Stanbridge EJ (1996) DNA damage and p53-mediated cell cycle arrest: a reevaluation. Proc Natl Acad Sci USA 93:15209–15214
47. Maréchal A, Zou L (2013) DNA damage sensing by the ATM and ATR kinases. Cold Spring Harb Perspect Biol 5:a012716
48. Miller V, Lin A, Kako F, Gabunia K, Kelemen S et al (2015) Microsecond-pulsed dielectric barrier discharge plasma stimulation of tissue macrophages for treatment of peripheral vascular disease. Phys Plasmas 22:122005
49. Ma Y, Ha CS, Hwang SW, Lee HJ, Kim GC et al (2014) Non-thermal atmospheric pressure plasma preferentially induces apoptosis in p53-mutated cancer cells by activating ROS stress-response pathways. PLoS ONE 9:e91947
50. Panngom K, Baik KY, Nam MK, Han JH, Rhim H et al (2013) Preferential killing of human lung cancer cell lines with mitochondrial dysfunction by nonthermal dielectric barrier discharge plasma. Cell Death Dis 4:e642
51. Ghimire B, Lamichhane P, Lim JS, Min B, Paneru R et al (2018) An atmospheric pressure plasma jet operated by injecting natural air. Appl Phys Lett 113:194101
52. Yan D, Talbot A, Nourmohammadi N, Cheng X, Canady J et al (2015) Principles of using cold atmospheric plasma stimulated media for cancer treatment. Sci Rep 5:18339
53. Kim SJ, Joh HM, Chung TH (2013) Production of intracellular reactive oxygen species and change of cell viability induced by atmospheric pressure plasma in normal and cancer cells. Appl Phys Lett 103:153705
54. Utsumi F, Kajiyama H, Nakamura K, Tanaka H, Mizuno M et al (2013) Effect of indirect nonequilibrium atmospheric pressure plasma on anti-proliferative activity against chronic chemo-resistant ovarian cancer cells in vitro and in vivo. PLoS ONE 8:e81576
55. Bauer G, Graves DB (2016) Mechanisms of selective antitumor action of cold atmospheric plasma-derived reactive oxygen and nitrogen species. Plasma Process Polym 13:1157–1178